

A NOVEL TWO PHASE HYBRID SWITCHED RELUCTANCE MOTOR/FIELD-ASSISTED GENERATOR: CONCEPT, SIMULATION, AND EXPERIMENTAL CONFIRMATION

E. Afjei and A.R. Siadatan*

*Department of Electrical Engineering, Shahid Beheshti University G.C.
P.O. Box 19839-63113, Tehran, Iran
e-afjei@sbu.ac.ir – a_siadatan@sbu.ac.ir*

*Corresponding Author

(Received: April 9, 2009 – Accepted in Revised Form: November 5, 2009)

Abstract The switched reluctance motor is a simple and robust machine, which has found application over a wide power and speed ranges in different shapes and geometries. This paper introduces a new configuration for a two phase unidirectional switched reluctance motor/field assisted generator. The proposed novel motor/generator consists of two magnetically independent stator and rotor sets (layers), where each stator set includes four salient poles with windings wrapped around them, while the rotor comprises of two salient poles with different arc lengths and no windings. There is a stationary reel, which has the field coils wrapped around it and is placed between the two-stator sets. In the motor mode of operation the two sets are connected independently. In this connection the stator poles in each layer can have both North and South Pole configurations. In the generator mode, the stator poles in one set can have either north or South Pole configuration while the stator poles in the other set (layer) have the opposite pole arrangements. In this format, the developed magnetic field from the stator poles travels to the rotor then to the rotor shaft and finally completes its path via the motor/generator housing. To evaluate the motor performance, two types of analysis, namely, the numerical technique and the experimental study have been utilized. In the numerical analysis, the finite element analysis is employed, where as in the experimental study, a proto-type motor has been built and tested.

Keywords Switched Reluctance Motor, Reluctance Motor/Generator, Hybrid Brushless Motor

چکیده موتور رلوکتانس سوئیچی یک ماشین ساده و قدرتمند با قابلیت استفاده در توان‌ها و سرعت‌های مختلفی می‌باشد که با ساختار و اشکال متفاوتی طراحی می‌شود. در این مقاله یک موتور ژنراتور میدان کمکی دوفاز تک جهت با ساختاری جدید ارائه می‌شود. موتور ژنراتور جدید شامل دو مجموعه استاتور و روتور است که از نظر مغناطیسی از یکدیگر مستقل می‌باشند، در حالی که هر مجموعه استاتور متشکل شده است از چهار قطب برجسته سیم پیچی شده و روتور آن شامل دو قطب برجسته با اندازه کمان‌های متفاوت و بدون سیم پیچی می‌باشد. در این ساختار، قرقره ثابتی وجود دارد که سیم پیچی میدان به دور آن پیچیده شده است و بین دو مجموعه استاتور قرار دارد. در حالت موتوری دو مجموعه به صورت مستقل اتصال یافته‌اند. در این اتصال، قطب‌های استاتور در هر لایه می‌تواند هر دو قطب شمال و جنوب را دارا باشد. در حالت ژنراتوری، قطب‌های استاتور در یک مجموعه دارای قطب شمال یا جنوب هستند، در حالی که در مجموعه دیگر قطب استاتور حالت دیگر را دارا می‌باشد. در این حالت، میدان مغناطیسی تولید شده از طریق استاتور به روتور و سپس شفت روتور هدایت می‌شود و در نهایت مسیر خود را از پوسته موتور ژنراتور می‌بندد. به منظور ارزیابی کارایی موتور، دو نوع تحلیل عددی و آزمایشگاهی انجام گرفته است. در تحلیل عددی، روش اجزای محدود به کار گرفته شده است و همچنین در تحلیل آزمایشگاهی یک نمونه آزمایشگاهی از موتور ژنراتور ساخته و تست شده است.

1. INTRODUCTION

Variable speed brushless motors as well as generators are gaining considerable attention for different high performance applications requiring low cost and maintenance. The switched reluctance

motor/generator is one of the challengers for low cost and simple structure in variable speed drive applications such as hybrid cars, home appliances, and wind turbines.

The two phase switched reluctance motor has gained much attention in the past few years due to

its simple motor construction [1-3] as well as the drive circuit which makes the two phase configuration very attractive in low cost, variable speed, and high volume applications such as home appliances and power tools. A two phase motor using common pole E-core structure is introduced in [4]. In this arrangement the E-core stator has three poles with two poles at the ends having windings and the center pole has no copper windings. In [5], a new two phase switched reluctance motor utilizing a governor for the control of excitation has been presented. In [6] different geometries have been proposed but all of them consist of six stator poles and three rotor poles with different pole arcs and some with variable air gaps. A detailed analysis of a 2-phase switched reluctance motor in which a significant component of the acoustic noise (ovalization) is suppressed or neutralized by means of a flux-switching transition has been discussed in [7]. High speed two phase switched reluctance motor with magnetic levitated rotor is presented for high speed applications in [8]. The design aspects of two-phase switched reluctance motors for fan-applications are being pointed out in [9]. It shows there is a trade-off between reduced costs of machine, converter and control which most likely results in an oversized motor.

Switched Reluctance Generator (SRG) is also an attractive solution for worldwide increasing demand of electrical energy [10]. It is low cost, fault tolerant with a rugged structure and operates with high efficiency over a wide speed range. Advantages of using SRG have been proved for some applications like starter/generator for gas turbine of aircrafts [11,12], windmill generator [13,14] and as an alternator for automotive applications [15]. The combination of switched reluctance motor with a field assisted generator looks a very promising arrangement for variable speed applications. Due to the rising demand for higher power and reduction of fuel consumption in cars, the concept of starter-generator has been investigated over the past several years. The application of electrical machines and drives systems in all-electric and hybrid-electric vehicles has been widely reported in recent years [16-19].

This paper is organized as follows. Section II explains the motor/generator construction. Section III contains the numerical analysis of the prototype

machine. Section IV includes the physical assembly of the machine as well as the experimental results obtained from the new hybrid switched reluctance motor/generator followed by conclusions in Section V.

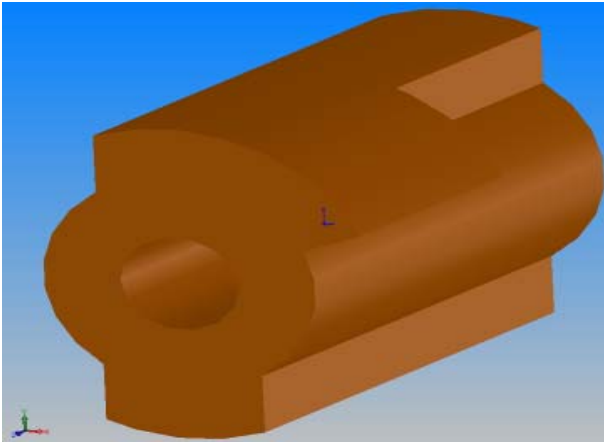
2. MOTOR/GENERATOR DESCRIPTION

The proposed novel motor/generator consists of two magnetically dependent stator and rotor sets (layers), where each stator set includes four salient poles having 45° arc length with coils wrapped around them while, the rotor comprises of two salient poles with different arc lengths. The rotor is shaped in such a way to produce starting torque as well as having rising inductance in all of 90° rotor arc length. The arc of each rotor pole is the same as stator pole (45°) in one side and twice as much in the other side.

The shape of rotor in each side is shown in Figure 1a, the actual rotor assembly is shown in Figure 1b, and finally, the stator laminations is shown in Figure 1c.

The two layers are exactly symmetrical with respect to a plane perpendicular to the middle of the motor shaft. Since this assembly is a two phase motor/generator; therefore, each layer consists of four stator poles and two rotor poles, respectively. In the motoring operation each layer operates independently, but in exact sequence with each other. In another words, each layer consists of a four by two reluctance motor configuration sharing a common shaft while operating in an exact sequence with respect to each other. There is a stationary reel, which has the field coils wrapped around it and is placed between the two-stator sets. This reel has a rotating cylindrical core, which guides the magnetic field. The magnetic flux produced by the coils travels through the guide and shaft to the rotor and then to the stator poles, and finally closes itself through the motor housing. Therefore, in the generator mode, one set of rotor poles is magnetically north while the other set is magnetically south. In this machine, the magnetic field has been induced to the rotor without using any brushes. A cut view of the motor/generator is shown in Figure 2.

In order to get a better view of the motor/generator



(a)



(b)



(c)

Figure 1. (a) Rotor shape, (b) actual rotor assembly and (c) stator laminations.

configuration, the complete motor/generator assembly is shown in Figure 3.

There are two stators and rotors sections placed on both sides of the field coil assembly which has the rotor shaft as its main core and two front/end caps plus the motor housing. Two sets of photo

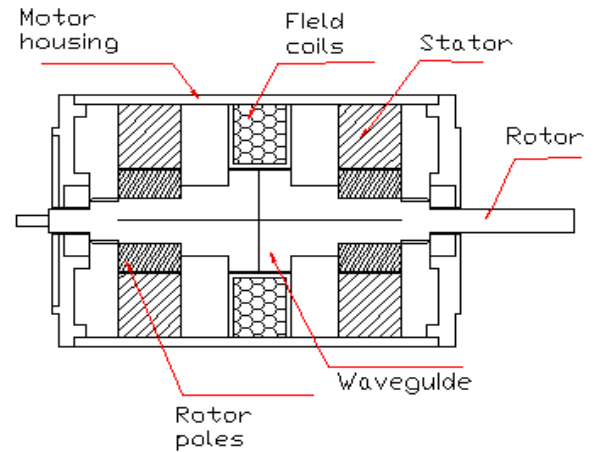


Figure 2. A cut view of the motor/generator.

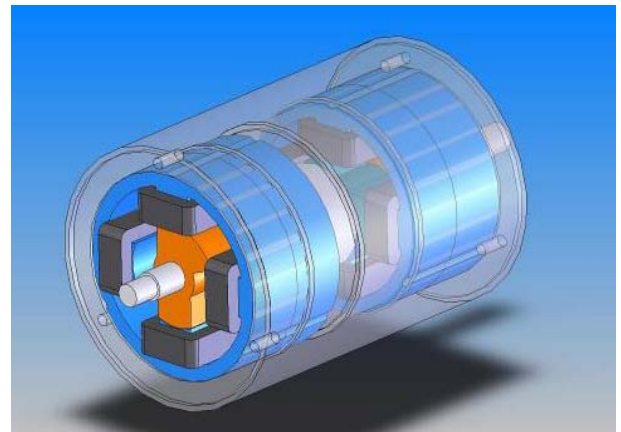


Figure 3. The complete motor/generator assembly.

interrupters are also placed in the back of the motor for the detection of rotor position. Two types of analysis namely numerical and experimental have been performed.

3. NUMERICAL ANALYSIS

The design of the motor becomes complicated due to complex geometry and material saturation. The reluctance variation of the motor has an important role on the performance; hence an accurate knowledge of the flux distribution inside the motor for different excitation currents and rotor positions

is essential for the prediction of motor performance. The motor can be highly saturated under normal operating conditions. To evaluate properly the motor design and performance a reliable model is required.

The finite element technique can be conveniently used to obtain the field distribution in and around the motor/generator.

There are two common methods for solving magnetic field problems one utilizes magnetic vector potential A and the other one employs electric vector potential T. The partial differential equation for the magnetic vector potential is given by;

$$-\frac{\partial}{\partial x}(\gamma \frac{\partial A}{\partial x}) - \frac{\partial}{\partial y}(\gamma \frac{\partial A}{\partial y}) - \frac{\partial}{\partial z}(\gamma \frac{\partial A}{\partial z}) = J \quad (1)$$

Where, A is the magnetic vector potential.

In the variational method (Ritz) the solution to (1) obtained by minimizing the following functional

$$F(A) = \frac{1}{2} \iiint_{\Omega} [\gamma (\frac{\partial A}{\partial x})^2 + \gamma (\frac{\partial A}{\partial y})^2 + \gamma (\frac{\partial A}{\partial z})^2] d\Omega - \iiint_{\Omega} J A d\Omega \quad (2)$$

Where Ω is the problem region of integration in this equation.

The field analysis has been performed using a Magnet CAD package which is based on the variational energy minimization technique to solve for the electric vector potential. In this method, electric vector potential known as T- Ω formulation in there T defined by;

$$J = \nabla \times T \quad (3)$$

From Maxwell's equation we have;

$$\nabla \times H = J = \nabla \times T \quad (4)$$

Then

$$\nabla \times (H - T) = 0 \quad (5)$$

Since the vector (H-T) can be expressed as the gradient of a scalar, i.e.

$$H = T - \nabla \Omega \quad (6)$$

Where in this formula Ω is a magnetic scalar potential.

and, Since

$$\nabla \times E = -\frac{\partial B}{\partial t} \quad (7)$$

Then;

$$\begin{aligned} \nabla \times E &= \nabla \times \left[\left(\frac{1}{\sigma} \right) \nabla \times T \right] = \\ -\frac{\partial B}{\partial t} &= -\mu_0 \mu_r \left(\frac{\partial}{\partial t} \right) (\nabla \times T) = -\mu_0 \mu_r \left(\frac{\partial T}{\partial t} \right) - \nabla \left(\frac{\partial \Omega}{\partial t} \right) \end{aligned} \quad (8)$$

Which finally reduces to the following two scalar equations

$$\nabla^2 T - \mu \sigma \left(\frac{\partial T}{\partial t} \right) = -\mu \sigma \nabla \left(\frac{\partial \Omega}{\partial t} \right) \quad (9)$$

and

$$\nabla^2 \Omega = 0 \quad (10)$$

When a three dimensional magnetic field problem is solved by A and V, the need to solve for all the three components of A arises, whereas using the T- Ω method, T can be simplified to produce a solution with only two components of T.

The motor specifications considered for the study is:

Stator core outer diameter	72 mm
Stator core inner diameter	62 mm
Stator arc	45 deg.
Air gap	0.25 mm
Rotor core outer diameter	39.5 mm
Rotor shaft diameter	10 mm
Rotor larger arc	90 deg.
Rotor smaller arc	45 deg.
Stack length	35 mm
Number of turns per pole	120
Number of turns for field coil	400

The analysis is carried out for the machine in two different modes of operation namely, motor mode and generator mode. In the motor mode of operation, the proper stator coils in each layer have been switched on while the field coil is turned off. In generator mode of operation two situations are considered, first is when the field coil assisting the power generation by carrying current and second is

when there is no field current in the center coil and power generation is carried out by energizing the proper stator coils during the negative inductance periods.

3.1. Motor Mode The motor/generator with and without the housing used in the numerical analysis are shown in Figure 4a-c. The 3-D field analysis has been performed using a commercial finite element package [20], which is based on the variational energy minimization technique to solve for the magnetic vector potential. The stator and rotor cores are made up of M-27 non-oriented silicon steel laminations [20].

Figure 5a,b show the magnetic flux density for non-aligned when the machine operates as a motor and each layer is operating independently.

Figure 6a-c show the magnetic flux density for

half aligned case when the machine operates as a motor and each layer is operating independently

Figures 7a-c show the magnetic flux density for aligned case when the machine operates as a motor and each layer is operating independently

The magnitude of magnetic flux density in the stator poles with energized coil starts from 0.5 Tesla at the beginning of rotor/stator pole alignment shown in Figure 5a and increases to 1.2 Tesla for half alignment shown in Figure 6a and then reaches to 1.45 Tesla at full alignment in Figure 7a. The same type of behavior for magnetic flux density can be seen in the motor yoke. The direction of magnetic flux travels from one energized stator pole winding to the yoke and then to the opposite stator pole as shown in Figures 5-7b. The flux pattern shaped over the motor housing shown in Figures 5-7c indicates some of the

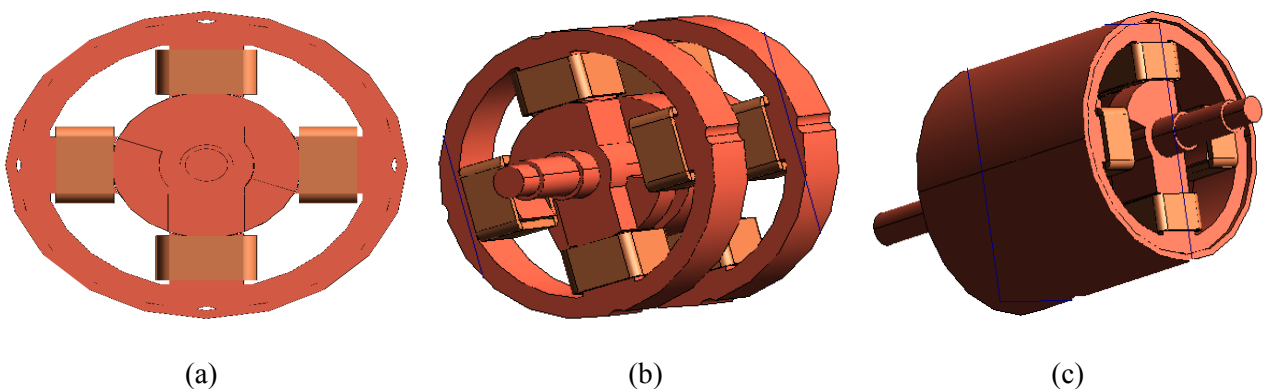


Figure 4. The motor/generator (a) front view, (b) without housing and (c) with housing.

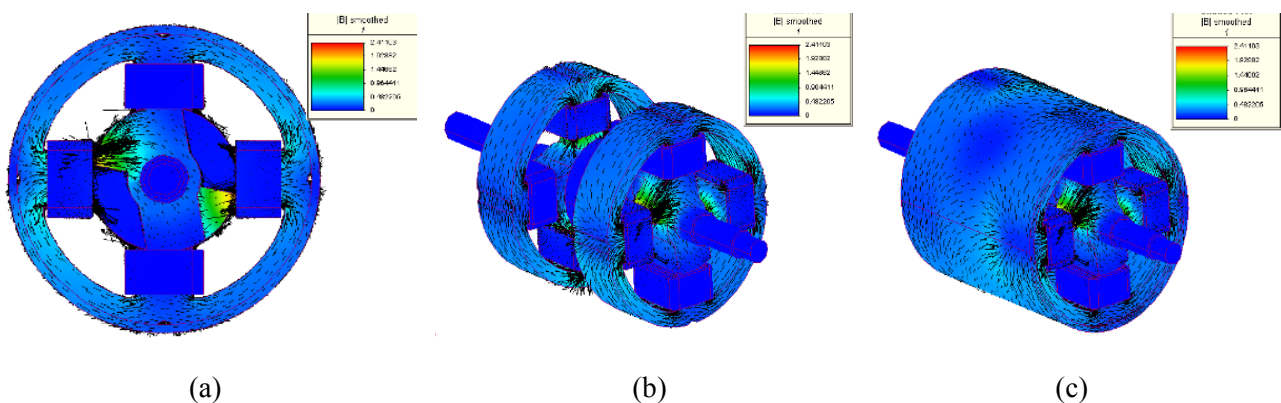


Figure 5. The 3-D magnetic field densities for non-aligned case (a,b and c).

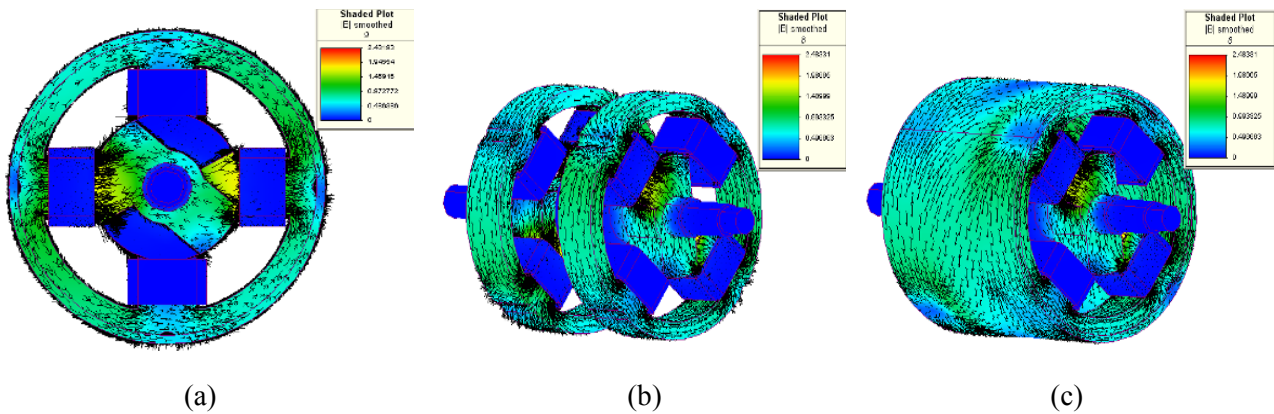


Figure 6. The magnetic flux density for half aligned case (a,b and c).

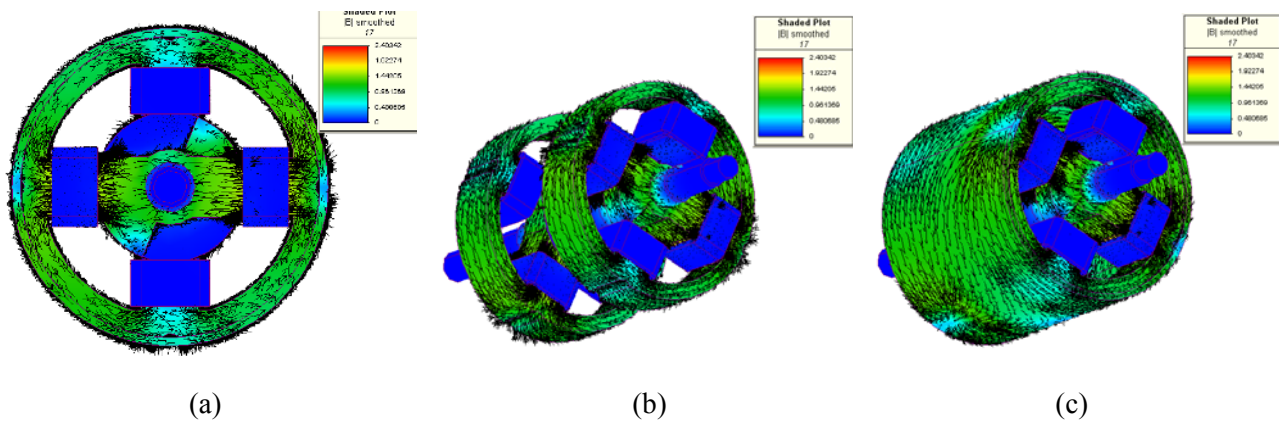


Figure 7. The 3-D magnetic field densities for non-aligned case (a,b and c).

magnetic field produced in the front layer travels through the motor housing to the back layer even though these two layers are operating independently.

The inductance has been defined as the ratio of each phase flux linkages to the exciting current (λ/I). Values based on this definition are presented in Figure 8 for the motor.

In the Figure 8, zero degree is considered to be as the unaligned case. The inductance profile shows steady increase as the rotor poles move into alignment with the stator poles, hence positive torque can be obtained from 0° to 90° of rotor arc.

The plot of static torque versus rotor positions developed by the hybrid reluctance motor/generator for a current of 3A is shown in Figure 9.

The torque starts at 0.1 N.m at the beginning and reaches its maximum of about 1.5 N.m at half

stator/rotor poles alignment and goes to zero at full alignment. The rising and falling of static torque which is mostly due to the square of motor phase current in this type of motor curves can be estimated adequately by two second degree polynomials.

3.2. Generator Mode In the field assisted generator mode of operation, the field coil between the two-stator sets is at 25 A. Figure 10a, shows the direction of the current in the center field coil as well as the magnetic flux density and Figures 10b-d show the magnetic flux density as well as the flux direction in the generator shaft, the rotor poles, rotor and stator assembly, and the generator housing, respectively.

In Figure 10a, the magnetic field produced by

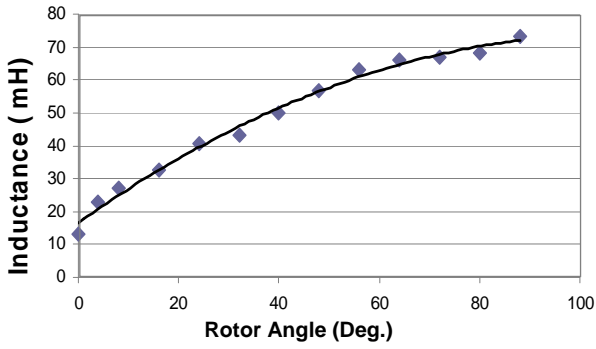


Figure 8. Terminal inductance vs. rotor position

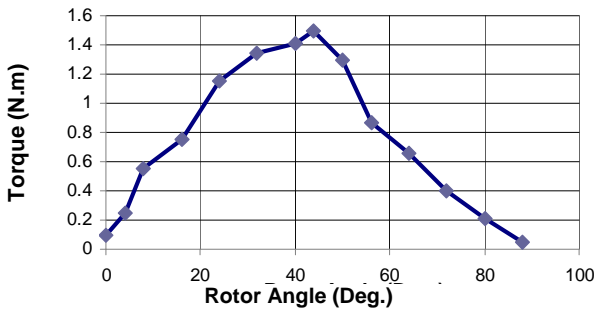


Figure 9. Static torque versus rotor positions.

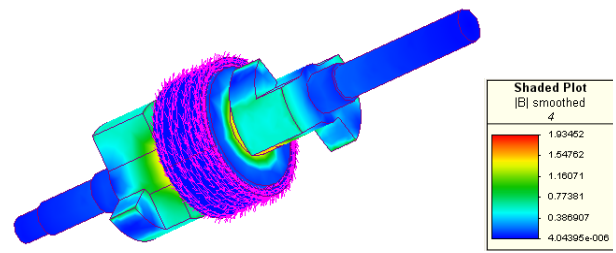
the coil travels through the shaft to the rotor poles and high magnetic flux densities has been produced under the rotor poles. The rotor poles in front and back have magnetically North and South Pole configurations, respectively. Figure 10b show the field coming out of the rotor pole tips perpendicularly and going into the respected stator poles. Finally, the magnetic flux pattern is shaped over the generator housing in which the flux travels from one set to the other set as is shown in Figure 10d.

Generated voltage can be calculated by;

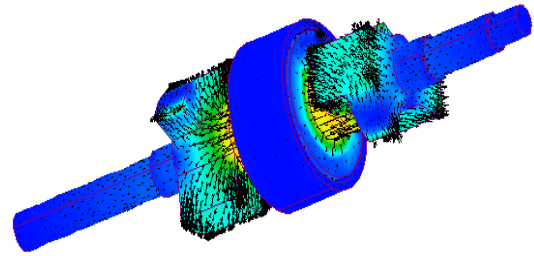
$$e_{ind} = \frac{\partial \lambda}{\partial t} = \frac{\partial (Li)}{\partial t} = L \frac{\partial i}{\partial t} + i \frac{\partial L}{\partial t} \quad (11)$$

Since current i is kept constant and $\frac{\partial \theta}{\partial t} = \omega$ then equation 11 can be rewritten as;

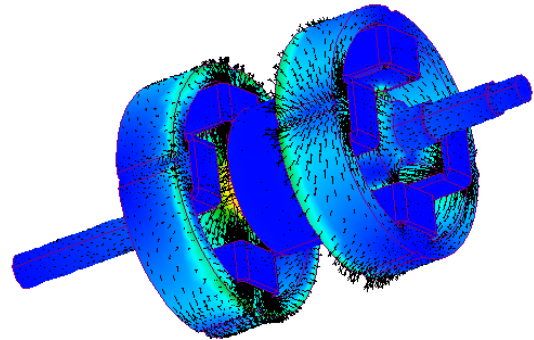
$$e_{ind} = i \frac{\partial L}{\partial \theta} \omega = N \frac{\partial \phi}{\partial \theta} \omega \quad (12)$$



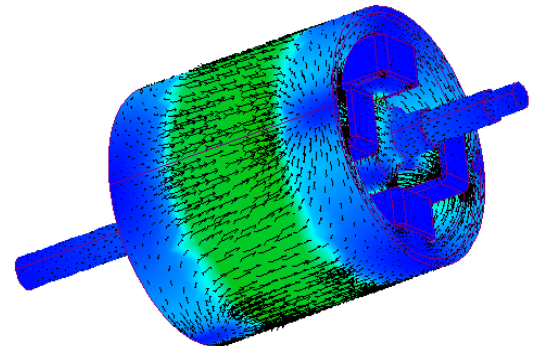
(a)



(b)



(c)



(d)

Figure 10. The current density, magnetic flux density and flux direction in: (a) The field coil and shaft, (b) the rotor poles, (c) rotor/stator assembly and (d) the generator housing.

Where, ω is motor angular speed in rad/s.

The flux linkage versus rotor position obtained by simulation for one of the stator pole windings is shown in Figure 11.

In order to estimate the shape of generated voltage, the flux linkage data points have been divided into five different segments. The different parts of Flux linkage curve can be explained in the following fashion, The first part is the segment before stator/rotor pole alignment, the second part starts at the beginning of stator/rotor pole alignment up to half aligned case, the third part is from half aligned to full aligned case, the fourth region begins at the start of unaligned rotor/stator pole up half un aligned case, and finally all the way to unaligned position.

A third order equation has been fitted through the data points for each part of the flux linkage curve. The equations are;

$$F(\theta) = 0.0001805\theta^3 + 0.004592\theta^2 + 0.03136\theta + 0.38$$

$$-15 < \theta < 5$$

$$F(\theta) = 3.182 \times 10^{-5}\theta^3 + 0.0007233\theta^2 + 0.2567\theta - 0.54$$

$$10 < \theta < 50$$

$$F(\theta) = 3.133 \times 10^{-5}\theta^3 - 0.008445\theta^2 + 0.7482\theta - 0.7$$

$$55 < \theta < 90$$

$$F(\theta) = 1.466 \times 10^{-5}\theta^3 - 0.007622\theta^2 + 0.8512\theta - 4.33$$

$$95 < \theta < 145$$

$$F(\theta) = -0.0001333\theta^3 + 0.0636\theta^2 - 10.11\theta - 492.2$$

$$150 < \theta < 165$$

The shape of induced voltage for a speed of 1000 rpm, using the different flux linkage curves obtained above is shown in Figure 12.

As seen from Figure 12, the maximum generated voltage has occurred at half aligned case.

The generated voltage in Figure 12 has different distinct parts which can be explained in the following manner. The first part is when the rotor pole moves closer to the stator pole and the generated voltage tends to increase. In the second segment, the rotor pole starts overlapping the stator pole and at this rotor position phase inductance jumps to a higher value and begins increasing as the

rotor pole aligns itself with stator pole, since the phase current is considered to be constant in the simulation therefore, the generated voltage rises as the phase inductance increases and finally reaches its maximum value at half alignment. It is worth mentioning that, at this rotor position, the pole belonging to the next phase starts its alignment therefore, some of the magnetic flux is directed to the this phase and the total magnetic flux density reduces in the first phase. In the next section, the first rotor pole is in half aligned position and going to full alignment and the second rotor pole moving into half aligned position, therefore the generated voltage drops due to the magnetic flux density reduction in that phase. Finally in the last part, the rotor pole is going into unaligned position and negative voltage is generated due to the negative slope of the flux linkage curve. The estimated average voltage is about 1 volt for the voltage curve shown in Figure 12.

At this point it is imperative to look at the field coil inductance curve to see how it varies as the rotor turns, because it can provide useful information in order to explain the difference in the simulated voltage curve with the experimental one. Figure 13 shows the calculated field inductance versus rotor position obtained by the ratio of flux linkage to the field current.

The maximum inductance occurs at every 45° since the field coil perceives two rotor pole sets which are positioned perpendicular to each other. When one rotor pole set is in full unaligned position with the stator poles the other rotor pole set is in full alignment with the other stator poles. In the above simulation, field current considered to be constant but in actual circuit the field voltage is constant and current will have some variation due to the changes in inductance value.

4. EXPERIMENTAL RESULTS

The motor has been fabricated and tested for performance and functionality in the laboratory. Figure 14a illustrates the different parts of the novel motor/generator before being assembled in the laboratory while Figure 14b shows the complete motor/generator. In the housing of the motor/generator assembly four grooves have been

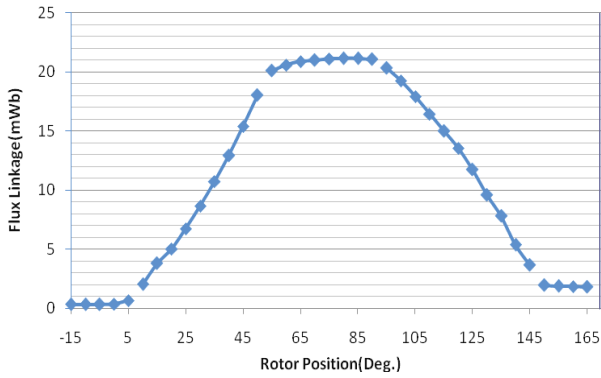


Figure 11. The flux linkage.

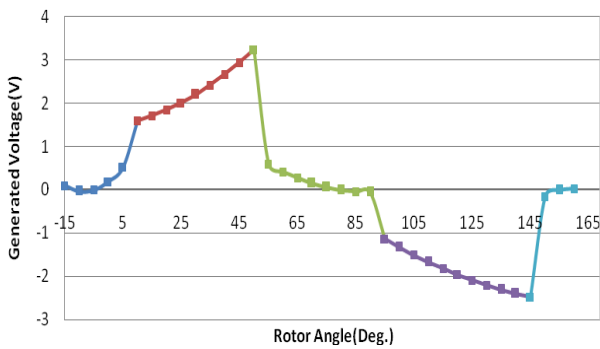


Figure 12. Induced voltage.

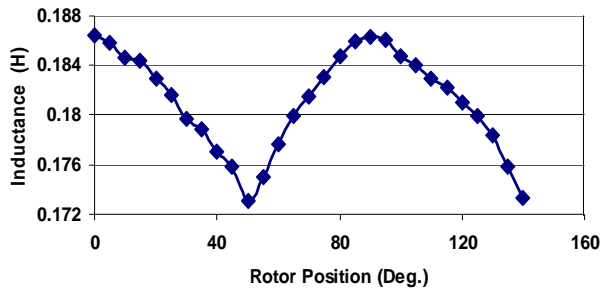


Figure 13. The calculated field inductance vs. rotor position.

cut out and filled with motor laminations in order to reduce the reluctance of the housing in such way that the magnetic flux is able to travel through the motor housing much easier.

The static torque of the motor was obtained by blocking the motor at different angle. The average

static torque for a rated current of 3 A was measured to be about 1.1 N. m over the rotor pole arc from 20° to 50°. It went to zero at the start of stator to rotor complete overlap. It was observed that the static torque shows lower value than computed which is expected, because the silicon steel sheet material used to build the motor is not quite what was used for the numerical analysis. Using a motor generator assembly, the dynamic torque for the motor versus speed has been measured by loading the motor. The torque-speed characteristic of the motor is shown in Figure 15. The power curve fitting has been used for the data points. The torque-speed characteristics of the motor are like a series dc motor. Figure 16 shows the torque versus current under different loads.

As seen from Figure 16, the torque is proportional to the square of motor current which resembles the dc series motor.

Figure 17 shows a set of opt-couplers with slotted disc as shaft position sensor is installed on the back of the motor in order to synchronize the proper firing of each phase transistor.

There are two opto-couplers, one for each layer and a slotted disc with two 90° openings, since each rotor arc is 90°.

Figure 18 shows the output signals coming from the two photo-interrupters mounted on the back of the motor.

There are four 90° pulses produced by the motor shaft position sensors in each rotation. When one signal is in a high state, the other one is in low state. Each pulse appears 2 times in one rotation for each phase since this is a two phase motor.

In the generator mode, the shaft of the motor/generator machine is connected to a motor to act as a prime mover. The speed of the motor is kept constant for various field currents; the resulting terminal voltage for only one pole winding after being rectified is shown in Figure 19.

In these figures curve fitting (power) has been used for better presentation of the data points.

The minimum voltage is about 0.87 volt at a field current of .25 A at 1000 rpm, which is within close agreement (less than 20%) with the computed average voltage resulted by simulation. One of the reasons for the production of the error is considering the field current to be constant in the simulation while it actually fluctuates in real generator unit.



(a)



(b)

Figure 14. (a) Different motor/generator parts and (b) The actual motor/generator.

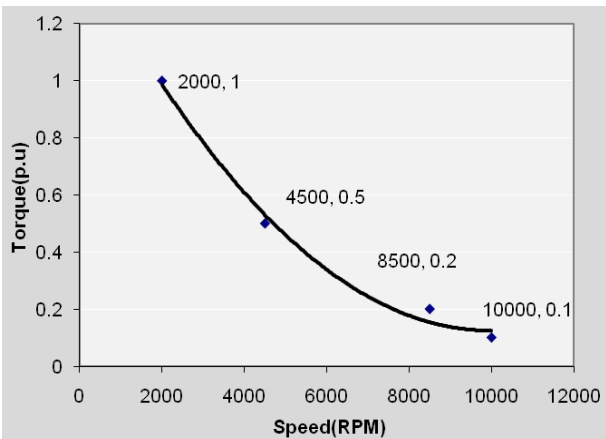


Figure 15. Torque versus speed.

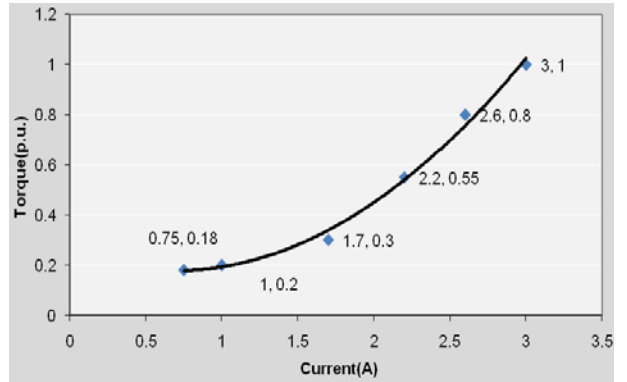


Figure 16. Torque versus current.

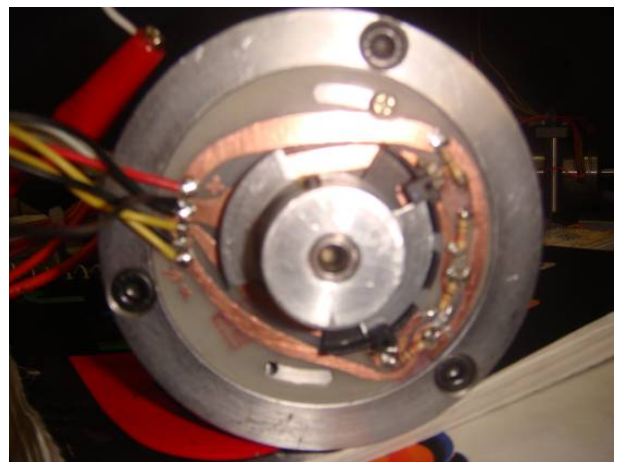


Figure 17. Direct shaft position sensors.

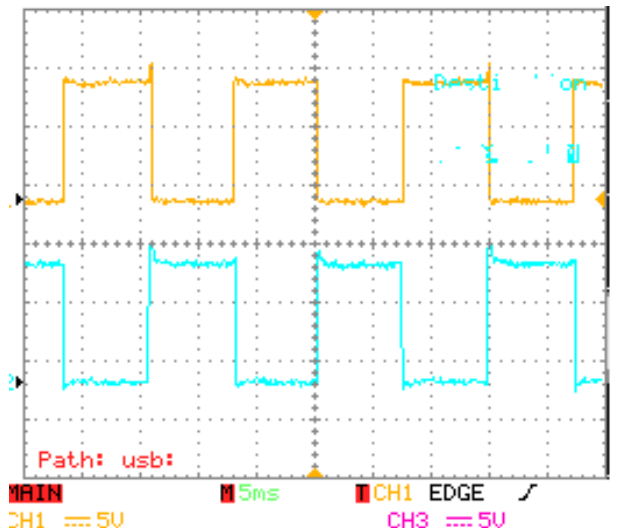


Figure 18. The output signals from the photo-interrupters.

The actual output voltage for one of the stator pole winding at no load is also shown in Figure 20.

The shape of this voltage waveform has some differences with the voltage waveform found numerically. One of the main reasons for these discrepancies is because of the current variation due to the changes in the field inductance value has not been not considered in the simulation. In order to be able to explain the shape of the generated voltage, the field current and one of the phase output voltage are shown together in Figures 21a,b respectively.

As the rotor turns the field current fluctuates around a dc value. This variation is due to the changes in the phase inductance value which in turn, affects the shape of output voltage.

When the rotor poles reach the stator poles, the output voltage rises to a maximum value (Figure 21b), and then starts decreasing as the rotor poles go into more alignment with stator poles, at the same time, the field current begins to decent due to production of high phase inductance value caused by stator/rotor poles alignment.

Due to the shape of the stator and rotor poles and saturation inside them, the generated output voltage has harmonics which is typical in this type of motor/generator unit.

5. CONCLUSION

In this paper a novel two phase hybrid motor/generator was fabricated in the laboratory. Some of the motor parameters numerically computed and experimentally measured and tested. The main objectives of this paper namely, introduction of a new two phase switched reluctance motor/generator configuration which can produce positive torque in all 360° rotor rotation in motoring mode with high durability has been achieved. The experimental findings support the simulated results with a difference of less than 20 %. The error in generated voltage is caused by considering the field current to be constant in the simulation of the generator unit while in experimental analysis the field current fluctuates due to variable reluctance nature of this motor/generator unit. The experimental analysis shows the functionality of the motor/generator in its new configuration, meaning, it has the ability and the potential of being used in hybrid vehicle or as a generator unit for wind turbine.

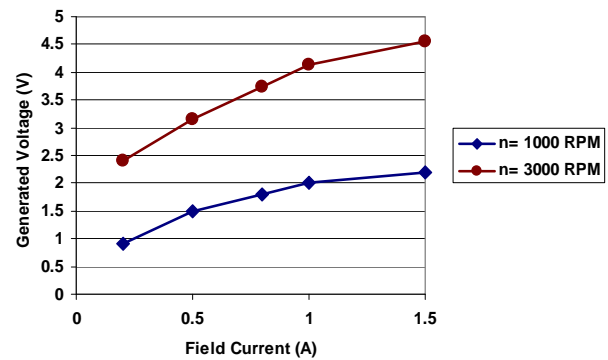


Figure 19. Generator terminal voltage vs. field current.

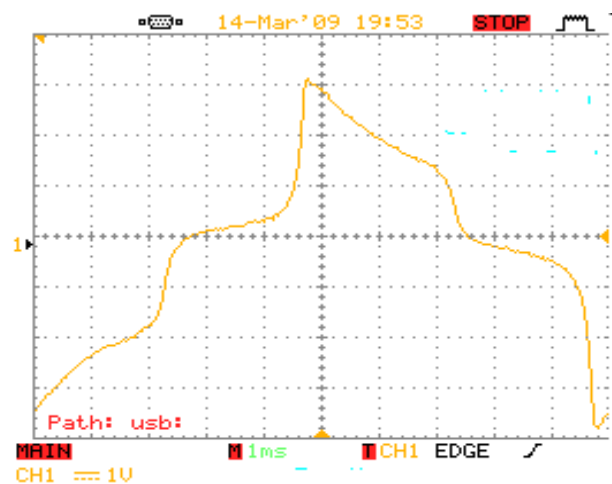


Figure 20. The actual output voltage for one of the stator pole winding at no load.

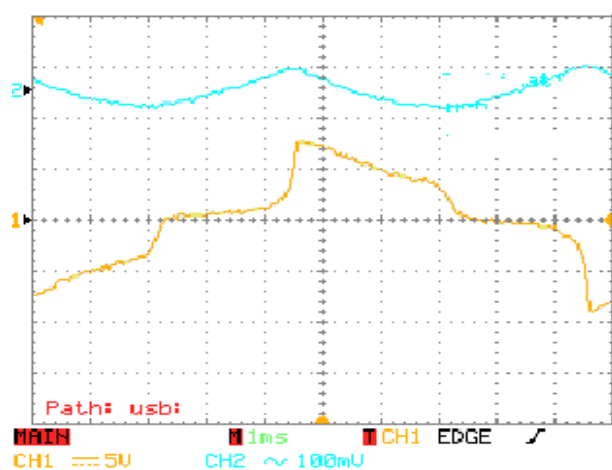


Figure 21. Voltage and current waveforms: (a) field current waveform and (b) output voltages waveform.

6. ACKNOWLEDGMENT

This work was supported by a grant from Shahid Beheshti University, power electronics and motor drives research center.

7. REFERENCES

1. Afjei, E. and Toliyat, H.A., "A Novel Multilayer Switched Reluctance Motor", *IEEE Transaction on Energy Conversion*, Vol. 17, No. 2, (2002), 217-221.
2. Torkaman, H. and Afjei, E., "Comprehensive Magnetic Field based study on Effects of Static Rotor Eccentricity in Switched Reluctance Motor Parameters Utilizing three Dimensional Finite Element", *Electromagnetics Journal, Taylor and Francis*, Vol. 29, (2009), 421-433.
3. Torkaman, H. and Afjei, E., "Comprehensive Study of 2-D and 3-D Finite Element Analysis of a Switched Reluctance Motor", *Journal of Applied science*, Vol. 8, No. 15, (2008), 2758-2763.
4. Lee, Ch., Krishnan, R. and Lobo, N.S., "New Designs of a Two-Phase E-Core Switched Reluctance Machine by Optimizing the Magnetic Structure for a Specific Application: Concept, Design, and Analysis", *IEEE, Industry Applications Society Annual Meeting*, (October 5-9, 2008), 1-8.
5. Afjei, E. Navi, B. and Ataei, S., "A New Two Phase Configuration for Switched Reluctance Motor with High Starting Torque", *IEEE, PED*, Thailand, (2007), 517-520.
6. Seok-Gyu O.h. and Krishnan, R., "Two-Phase SRM with Flux-Reversal-Free Stator: Concept, Analysis, Design, and Experimental Verification", *IEEE Transactions on Industry Applications*, Vol. 43, No. 5, (September/October 2007), 1247-1257.
7. Pengov, W., Hendershot, J.R. and Miller, T.H.E., "A New Low-Noise Two-Phase Switched Reluctance Motor", *IEEE International Conference Electric Machines and Drives*, (May 15-18, 2005), 1281-1284.
8. Sun, L., Yang, G. and Feng, Qi., "Study on the Rotor Levitation of one High Speed Switched Reluctance Motor", *IEEE Conference on Industrial Electronics, IECON*, (November 6-10, 2006), 1322-1325.
9. Piedler, R.W. and Doncker, De., "Designing Low-Cost Switched Reluctance Drives for Fan-Applications", *IEEE Second International Conference on Power Electronics, Machines and Drives*, Vol. 2, No. 31, (March 2-April 2004), 758-762.
10. Radun, A., "Generating with the Switched-Reluctance Motor", In Proc. IEEE APEC'94, (1994), 41-47.
11. Mac Minn, S.R. and Sember, J.W., "Control of a Switched-Reluctance Aircraft Starter-Generator Over a Very Wide Speed Range", *In Proc. Intersociety Energy Conversion Engineering Conf.*, (1989), 631-638.
12. Ferreira, C.A., Jones, S.R., Heglund, W.S. and Jones, W.D., "Detailed Design of a 30-kW Switched Reluctance Starter/Generator System for a Gas Turbine Engine Application", *Industry Applications Society Annual Meeting*, Vol. 1, (1993), 97-105.
13. Mueller, M.A., "Design of Low Speed Switched Reluctance Machines for Wind Energy Converters", *Electrical Machines and Drives, Ninth International Conference on (Conf. Publ. No. 468)*, (September 1-3, 1999), 60-64
14. Cardenas, R., Ray, W.F. and Asher, G.M., "Switched Reluctance Generators for wind Energy Applications", *In Proc. IEEE PESC'95*, (1995), 559-564.
15. Fahimi, B., Emadi, A. and Sepe, R., "A Switched Reluctance Machine Based Starter/Alternator for More Electric cars" Energy Conversion, *IEEE Transactions on Energy Conversion*, Vol. 19, (March 2004), 116-124.
16. Rahman, K.M., Fahimi, B., Suresh, G., Rajarathnam, A.V. and Ehsani, M., "Advantages of Switched Reluctance Motor Applications to EV and HEV: Design and Control Issues", *IEEE Trans. Industry. Applications*, Vol. 36, (January-February 2000), 111-121.
17. Emadi, A., "Low-Voltage Switched Reluctance Machine Based Traction Systems for Lightly Hybridized Vehicles", *Society of Automotive Engineers*, (2001), 1-7.
18. Koch, J.L., Probst, G. and Schafer, H., "The Integrated Starter Generator as Part of the Power Train Management", *Aachener Kollequium Fahrzeug-und Motoren Technik*, (2000), 11-11.
19. Afjei, E., Hashemipour, O., Saati, M.A. and Nezamabadi, M.M., "A New Hybrid Brushless dc Motor/Generator without Permanent Magnet: *International Journal of Engineering, Transactions B: Applications*, Vol. 20, No. 1, (April 2007), 77-86.
20. Magnet CAD Package: "User Manual", Infolytica Corporation Ltd., Montreal, Canada, (2006).